Western blotting

Total protein extracts were prepared from MEFs with RIPA lysis buffer. For western blots, 50 μg of protein extracts per lane were subjected to electrophoresis, transferred to poly(vinylidene difluoride) membranes (Millipore) and immunoblotted with anti-Notch4 (H-225; Santa Cruz), Notch1 (C-20; Santa Cruz) and anti-cyclin E (M-20; Santa Cruz), presenilin-1 (N-19; Santa Cruz), c-Jun (H-79; Santa Cruz), p53 (CM5; Novocastra Laboratories) and Aurora-A (BD Transduction Laboratories) antibodies; as control, the same membranes were stripped and immunoblotted again with anti-β-actin antibody (AC-15; Sigma). The membranes were washed and treated with rat anti-specific IgG^{κ}-chain secondary antibody conjugated to horseradish peroxidase (Amersham Pharmacia). The antigen–antibody reactions were revealed by using an enhanced chemiluminesence assay (ECL; Amersham Pharmacia) and exposed to enhanced chemiluminesence film.

Statistical analysis

Difference in frequency of LOH between $p53^{+/-}$ and $p53^{-/-}$ was assessed by genome-wide permutation testing. The Kaplan–Meier method was used to compare the survival time after irradiation between different groups of genotypes of mice with the use of the SPSS statistical package.

Received 22 July; accepted 3 November 2004; doi:10.1038/nature03155.

1. Rajagopalan, H. *et al.* Inactivation of hCDC4 can cause chromosomal instability. *Nature* **428,** 77–81 (2004).
2. Donehower, L. A. *et al.* Mice deficient for p53 are developmentally normal but susceptible to spontaneous tumours. *Nature* **356,** 215–221 (1992).
3. Kemp, C. J., Wheldon, T. & Balmain, A. p53-deficient mice are extremely susceptible to radiation-induced tumorigenesis. *Nature Genet.* **8,** 66–69 (1994).
4. Grigorian, M. *et al.* Tumour suppressor p53 protein is a new target for the metastasis-associated Mts1/S100A4 protein: functional consequences of their interaction. *J. Biol. Chem.* **276,** 22699–22708 (2001).
5. Browes, C., Rowe, J., Brown, A. & Montano, X. Analysis of trk A and p53 association. *FEBS Lett.* **497,** 20–25 (2001).
6. Strohmaier, H. *et al.* Human F-box protein hCdc4 targets cyclin E for proteolysis and is mutated in a breast cancer cell line. *Nature* **413,** 316–322 (2001).
7. Moberg, K. H., Bell, D. W., Wahrer, D. C., Haber, D. A. & Hariharan, I. K. Archipelago regulates cyclin E levels in *Drosophila* and is mutated in human cancer cell lines. *Nature* **413,** 311–316 (2001).
8. Spruck, C. H. *et al.* hCDC4 gene mutations in endometrial cancer. *Cancer Res.* **62,** 4535–4539 (2002).
9. Calhoun, E. S. *et al.* BRAF and FBXW7 (CDC4, FBW7, AGO, SEL10) mutations in distinct subsets of pancreatic cancer: potential therapeutic targets. *Am. J. Pathol.* **163,** 1255–1260 (2003).
10. Koepp, D. M. *et al.* Phosphorylation-dependent ubiquitination of cyclin E by the SCFFbw7 ubiquitin ligase. *Science* **294,** 173–177 (2001).
11. Wu, G. *et al.* SEL-10 is an inhibitor of notch signaling that targets notch for ubiquitin-mediated protein degradation. *Mol. Cell. Biol.* **21,** 7403–7415 (2001).
12. Oberg, C. *et al.* The Notch intracellular domain is ubiquitinated and negatively regulated by the mammalian Sel-10 homolog. *J. Biol. Chem.* **276,** 35847–35853 (2001).
13. Gupta-Rossi, N. *et al.* Functional interaction between SEL-10, an F-box protein, and the nuclear form of activated Notch1 receptor. *J. Biol. Chem.* **276,** 34371–34378 (2001).
14. Hoh, J. *et al.* The p53MH algorithm and its application in detecting p53-responsive genes. *Proc. Natl Acad. Sci. USA* **99,** 8467–8472 (2002).
15. Kimura, T., Gotoh, M., Nakamura, Y. & Arakawa, H. hCDC4b, a regulator of cyclin E, as a direct transcriptional target of p53. *Cancer Sci.* **94,** 431–436 (2003).
16. Tsunematsu, R. *et al.* Mouse Fbw7/Sel-10/Cdc4 is required for notch degradation during vascular development. *J. Biol. Chem.* **279,** 9417–9423 (2004).
17. Tetzlaff, M. T. *et al.* Defective cardiovascular development and elevated cyclin E and Notch proteins in mice lacking the Fbw7 F-box protein. *Proc. Natl Acad. Sci. USA* **101,** 3338–3345 (2004).
18. Ye, Q., Shieh, J. H., Morrone, G. & Moore, M. A. Expression of constitutively active Notch4 (Int-3) modulates myeloid proliferation and differentiation and promotes expansion of hematopoietic progenitors. *Leukemia* **18,** 777–787 (2004).
19. Zhou, H. *et al.* Tumour amplified kinase STK15/BTAK induces centrosome amplification, aneuploidy and transformation. *Nature Genet.* **20,** 189–193 (1998).
20. Miyoshi, Y., Iwao, K., Egawa, C. & Noguchi, S. Association of centrosomal kinase STK15/BTAK mRNA expression with chromosomal instability in human breast cancers. *Int. J. Cancer* **92,** 370–373 (2001).
21. Meraldi, P., Honda, R. & Nigg, E. A. Aurora-A overexpression reveals tetraploidization as a major route to centrosome amplification in p53−/− cells. *EMBO J.* **21,** 483–492 (2002).
22. Nateri, A. S., Riera-Sans, L., Da Costa, C. & Behrens, A. The ubiquitin ligase SCFFbw7 antagonizes apoptotic JNK signaling. *Science* **303,** 1374–1378 (2004).
23. Fero, M. L., Randel, E., Gurley, K. E., Roberts, J. M. & Kemp, C. J. The murine gene p27Kip1 is haplo-insufficient for tumour suppression. *Nature* **396,** 177–180 (1998).
24. Tang, B. *et al.* Transforming growth factor-β1 is a new form of tumour suppressor with true haploid insufficiency. *Nature Med.* **4,** 802–807 (1998).
25. Artandi, S. E. *et al.* Telomere dysfunction promotes non-reciprocal translocations and epithelial cancers in mice. *Nature* **406,** 641–645 (2000).
26. Liu, G. *et al.* High metastatic potential in mice inheriting a targeted p53 missense mutation. *Proc. Natl Acad. Sci. USA* **97,** 4174–4179 (2000).
27. Hanks, S. *et al.* Constitutional aneuploidy and cancer predisposition caused by biallelic mutations in *BUB1B*. *Nature Genet.* **36,** 1159–1161 (2004).
28. Frenkel, J. *et al.* Accentuated apoptosis in normally developing p53 knockout mouse embryos following genotoxic stress. *Oncogene* **18,** 2901–2907 (1999).
29. Linardopoulos, S. *et al.* Deletion and altered regulation of p16INK4a and p15INK4b in undifferentiated mouse skin tumors. *Cancer Res.* **55,** 5168–5172 (1995).
30. Brummelkamp, T. R., Bernards, R. & Agami, R. A system for stable expression of short interfering RNAs in mammalian cells. *Science* **296,** 550–553 (2002).

Supplementary Information accompanies the paper on **www.nature.com/nature**.

Acknowledgements We thank the staff of the CRUK Beatson Institute and UCSF Comprehensive Cancer Center animal house for animal husbandry; L. Heath (Laboratory Animal Resource Center, UCSF) for analysing the histological slides from tumors; and J. Hoh (Laboratories of Statistical Genetics and Cancer Biology of The Rockefeller University, New York, USA) for providing the p53MH algorithm program. The UCSF Cancer Center Genome Core was essential for the sequencing and study design of the Taqman assay. These studies were initially supported by the Commission of the European Communities and the Cancer Research Campaign (UK), and subsequently by an NCI grant and a DOE grant to A.B. J.H.M. is the recipient of a Leukemia & Lymphoma Society Fellowship. J.P.L. has a Fellowship from the 'Ministerio de Educacion y Ciencia' of Spain. A.B. is the recipient of the Barbara Bass Bakar Chair in Cancer Genetics.

Competing interests statement The authors declare that they have no competing financial interests.

Correspondence and requests for materials should be addressed to A.B. (abalmain@cc.ucsf.edu).

Rubisco without the Calvin cycle improves the carbon efficiency of developing green seeds

Jörg Schwender, Fernando Goffman, John B. Ohlrogge & Yair Shachar-Hill

Plant Biology Department, Michigan State University, East Lansing, Michigan 48824, USA

Efficient storage of carbon in seeds is crucial to plant fitness and to agricultural productivity. Oil is a major reserve material in most seeds[1], and these oils provide the largest source of renewable reduced carbon chains available from nature. However, the conversion of carbohydrate to oil through glycolysis results in the loss of one-third of the carbon as CO_2. Here we show that, in developing embryos of *Brassica napus* L. (oilseed rape), Rubisco (ribulose 1,5-bisphosphate carboxylase/oxygenase) acts without the Calvin cycle[2] and in a previously undescribed metabolic context to increase the efficiency of carbon use during the formation of oil. In comparison with glycolysis, the metabolic conversion we describe provides 20% more acetyl-CoA for fatty-acid synthesis and results in 40% less loss of carbon as CO_2. Our conclusions are based on measurements of mass balance, enzyme activity and stable isotope labelling, as well as an analysis of elementary flux modes.

During embryogenesis, seeds receive carbon precursors from the mother plant for the synthesis of storage products. In oilseeds such as *B. napus*, the dominant metabolic flux is the conversion of sugars into triacylglycerols[3], resulting in more than 60% of the carbon being stored as oil (about 45% of dry weight). In described pathways for plant oil synthesis, sucrose is converted into pyruvate through glycolysis, which is then transformed into acetyl-CoA, the precursor of fatty-acid biosynthesis[4]. This conversion of sugars to oil entails the loss of one carbon as CO_2 at the pyruvate dehydrogenase (PDH) reaction for each two-carbon acetyl-CoA unit produced for oil synthesis (Fig. 1b). This loss of carbon seems to make oil storage less advantageous for seeds and raises the question why so many plant species use oil as their primary reserve in seeds and whether there is a more efficient way of transforming carbohydrates to oil. Because many seeds are green and have photosystems, even the decreased amount of light that penetrates the fruit wall[5] can provide reductant and ATP that may expand the range of pathways available for storage product synthesis.

To measure the efficiency of carbon utilization during oilseed development, *B. napus* embryos were fed uniformly ^{14}C-labelled carbon sources, and their conversion into oil, protein, carbo-

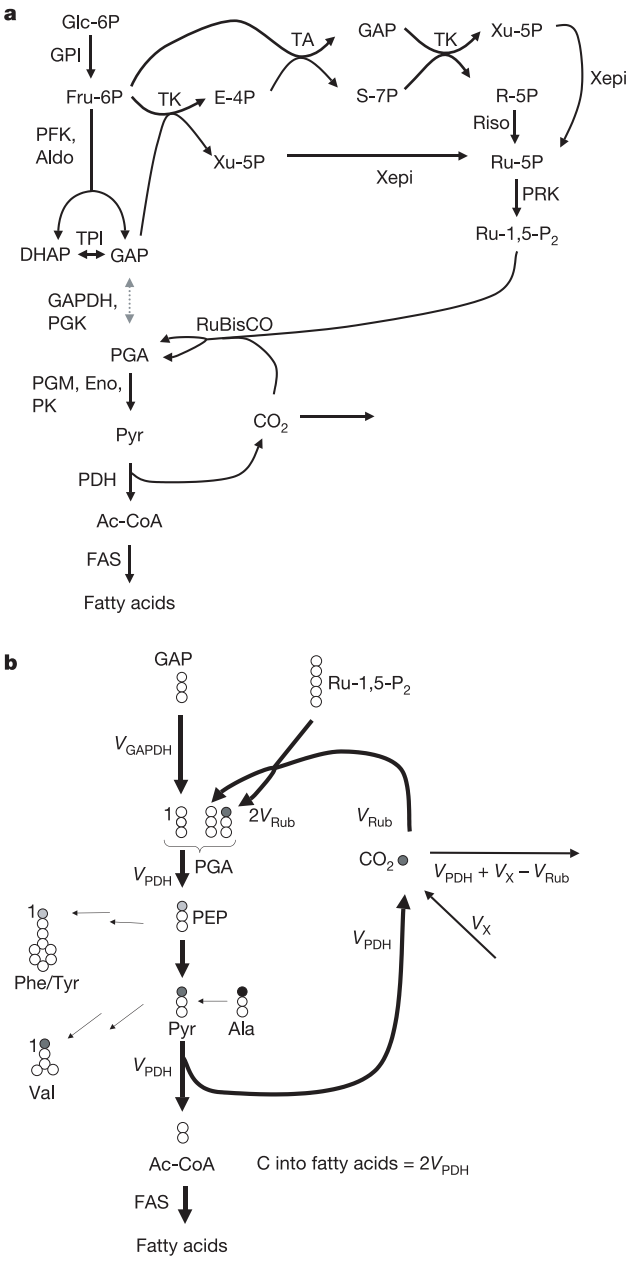

Figure 1 Metabolic transformation of sugars into fatty acids. **a**, Conversion of hexose phosphate to pentose phosphate through the non-oxidative steps of the pentose phosphate pathway and the subsequent formation of PGA by Rubisco bypasses the glycolytic enzymes glyceraldehyde-3-phosphate dehydrogenase and phosphoglycerate kinase while recycling half of the CO_2 released by PDH. PGA is then further processed to pyruvate, acetyl-CoA and fatty acids. **b**, Part of **a** expanded to indicate carbon skeletons and to define relationships between V_{PDH} (flux through PDH complex); V_X (additional CO_2 production by the OPPP, the TCA, and so on); V_{Rub} (refixation by Rubisco). Metabolites: Ac-CoA, acetyl coenzyme-A; DHAP, dihydroxyacetone-3-phosphate; E4P, erythrose-4-phosphate; Fru-6P, fructose-6-phosphate; GAP, glyceraldehydes-3-phosphate; Glc-6P, glucose-6-phosphate; PGA, 3-phosphoglyceric acid; Pyr, pyruvate; R-5P, ribose-5-phosphate; Ru-1,5-P_2, ribulose-1,5-bisphosphate; Ru-5P, ribulose-5-phosphate; S-7P, sedoheptulose-7-phosphate; Xu-5P, xylulose-5-phosphate. Enzymes: Aldo, fructose bisphosphate aldolase; Eno, 2-phosphoglycerate enolase; Xepi, xylulose-5-phosphate epimerase; FAS, fatty-acid synthase, PGM, phosphoglyceromutase; GAPDH, glyceraldehyde-3-phosphate dehydrogenase; GPI, phosphoglucose isomerase; Riso, ribose-5-phosphate isomerase; PDH, pyruvate dehydrogenase; PFK, phosphofructokinase; PK, pyruvate kinase, PGK, phosphoglycerate kinase; PRK, phosphoribulokinase; TA, transaldolase; TK, transketolase; TPI, triose phosphate isomerase.

hydrates and CO_2 was determined. Table 1 shows the partitioning of carbon into different biomass fractions and the proportion of carbon liberated as CO_2. The measured ratio of carbon stored in oil to carbon liberated as CO_2 was close to 3:1, which was substantially higher than expected. The formation of acetyl-CoA from pyruvate by PDH results in a ratio of 2:1, and CO_2 production from additional metabolic activities (such as the oxidative pentose-phosphate pathway (OPPP)[6] and the tricarboxylic acid (TCA) cycle[3]) would decrease the ratio further. Thus, considerably less CO_2 was produced than expected from the amount of oil formed.

We considered whether the decreased CO_2 emission in light was due to its refixation by means of phosphoenolpyruvate carboxylase or pyruvate carboxylase. The product, oxaloacetate, could be converted into amino acids and stored in proteins or possibly secreted from the embryo (for example, in reduced form as malate). However, on the basis of the amino acid composition of *B. napus* embryos, recovery of CO_2 through oxaloacetate into seed protein can account for only about 4% of the CO_2 released by PDH (see Supplementary Information I). In addition, no export of malate or other such fixation products from embryos was detected (NMR data not shown). The observation of substantial Rubisco activity in *B. napus* seeds[5,7] indicates that the reassimilation of CO_2 by the Calvin cycle might explain the increased efficiency of carbon use. The catalytic capacities of both Rubisco and phosphoribulokinase in developing *B. napus* seeds are sufficient to potentially fix all the CO_2 released by PDH[7], and seed CO_2 levels[8] saturate Rubisco carboxylase activity and prevent its oxygenase activity.

The results of labelling experiments show that CO_2 fixation by Rubisco is indeed active but that the Calvin cycle is not functional. Developing embryos were cultured in an atmosphere containing 2% $^{13}CO_2$—a concentration similar to the CO_2 levels that we and others[5] measured in the gas-filled spaces, or locules, of developing siliques. Alternatively, alanine in the medium was replaced with [1-^{13}C]alanine or [U-$^{13}C_3$]alanine, which results in the release of $^{13}CO_2$ internally through the action of alanine aminotransferase and then PDH. In both experiments the distribution of ^{13}C in amino acids and fatty acids shows that only the C1 carbon position of 3-phosphoglyceric acid (PGA) became labelled (Table 2). This is where CO_2 fixed by Rubisco is located; fatty acids, which are derived from C2 and C3 of PGA (Fig. 1b), were labelled to extremely low levels (Table 2). This labelling pattern is incompatible with flux through the Calvin cycle, in which the cyclic regeneration of ribulose-1,5-bisphosphate from PGA results in label from CO_2 being distributed into all carbon positions of the cycle's intermediates (including PGA)[2]. We therefore concluded that although Rubisco is active in fixing CO_2 by the usual carboxylation reaction, it is not operating as part of the Calvin cycle but in a different context.

On the basis of the above results we conclude that Rubisco operates as part of a previously undescribed metabolic route between carbohydrate and oil (Fig. 1a). This involves three stages: first, the conversion of hexose phosphates to ribulose-1,5-bisphosphate by the non-oxidative reactions of the OPPP together with phosphoribulokinase; second, the conversion of ribulose-1,5-bisphosphate and CO_2 (most of which is produced by PDH[3]) to PGA by Rubisco; and third, the metabolism of PGA to pyruvate and thence to fatty acids (Fig. 1a). The net carbon stoichiometry of this conversion (for details see Supplementary Information II) is

$$5 \text{ hexose phosphate} \rightarrow 6 \text{ pentose phosphate} \rightarrow 12 \text{ acetyl-CoA} + 6\ CO_2$$

By contrast, the conversion of the same amount of hexose phosphates through glycolysis is

$$5 \text{ hexose phosphate} \rightarrow 10 \text{ Acetyl-CoA} + 10\ CO_2$$

Thus, Rubisco, together with the non-oxidative enzymes of the

Table 1 **Observed and expected biomass production and CO_2 release by *B. napus* embryos in culture**

Metabolic sink	Percentage of carbon observed	Percentage of carbon expected by conventional pathways
Oil	49.7 ± 2.8	<44.9*
Protein, starch, cell wall, etc.	32.7 ± 2.3	32.7
CO_2 released	17.6 ± 2.2	>22.4*
Ratio of carbon in oil to CO_2 released	2.9 ± 0.3	<2.0

Aseptically isolated embryos in the early phase of storage accumulation were grown in liquid culture for 3 days at a light intensity of 50 $\mu mol\,m^{-2}\,s^{-1}$, with glucose, sucrose, glutamate and alanine as ^{14}C-labelled substrates. Standard deviations are given for $n = 5$ experiments.
*Assuming that CO_2 is produced only for oil synthesis (PDH reaction), the carbon fractions of oil and CO_2 are expected to be in the ratio 2:1. This value is a minimum because, in addition to PDH, the OPPP and the TCA cycle produce CO_2 (see the text).

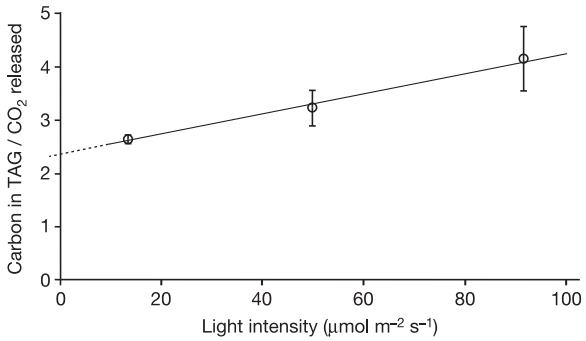

Figure 2 Light-dependent ratio of oil synthesis and CO_2 production. Embryos were grown at three different light levels for 24 h in closed culture flasks[6,9]. After 24 h the CO_2 concentration inside the flasks was determined with an infrared gas analyser[8], and the lipid content of embryo tissue was analysed by gas chromatography. Results are means ± standard error ($n = 3$). TAG, triacylglycerol.

pentose phosphate pathway, allows the conversion of carbohydrate into 20% more acetyl-CoA and therefore oil than does glycolysis, with 40% less carbon lost as CO_2. This metabolic route is consistent with the mass balance data shown in Table 1, which, given the absence of substantial other CO_2 refixing mechanisms, are incompatible with the glycolytic route. Although Rubisco has a central function in the metabolic route that we describe, net fixation of CO_2 does not occur because the CO_2 fixed by Rubisco is subsequently released by PDH. The increase in carbon economy is therefore achieved only through the combined activity of Rubisco with the non-oxidative reactions of the pentose phosphate pathway.

We used two independent approaches to estimate how large a contribution this metabolic route makes to seed oil synthesis (at a light intensity of 50 $\mu mol\,m^{-2}\,s^{-1}$).

First, the carbon balance of the embryo was used. The ratio of fatty-acid synthesis to CO_2 release can be formulated as (see Fig. 1b)

$$R = \frac{\text{carbon stored in fatty acids}}{\text{carbon released as } CO_2} = \frac{2V_{PDH}}{V_{PDH} + V_X - V_{RuB}} \quad (1)$$

where V_{PDH} and V_{RuB} are the fluxes through PDH and Rubisco respectively and V_X is the net CO_2 production due to the rest of metabolism (primarily the OPPP and the TCA cycle). This can be recast to allow V_{RuB} to be deduced from measurements of R and V_X:

$$V_{RuB} = V_X + V_{PDH}\left(1 - \frac{2}{R}\right) \quad (2)$$

We measured R to be 2.9 (Table 1) and determined that V_X is positive and small (see refs 3 and 5 and Supplementary Information). Accordingly, $V_{RuB} > 0.31V_{PDH}$. Because the great majority of PGA is converted to pyruvate and thence to acetyl-CoA[9], the total rate of PGA production is very close to V_{PDH}. Because two PGA molecules are produced by the Rubisco carboxylase reaction, the rate of PGA production by Rubisco is $2V_{RuB}$. Thus, Rubisco is responsible for more than 62% of the total PGA production (46–75%, considering the range for R (Table 1)).

Second, we supplied [1-^{13}C]Ala and [U-$^{13}C_3$]Ala to developing embryos, which results in the release of $^{13}CO_2$ internally through the PDH reaction. The flux through Rubisco was estimated from the level of ^{13}C in the C1 position of PGA-derived amino acids that arises from the direct incorporation of $^{13}CO_2$ by Rubisco. In the absence of flow round the Calvin cycle, the PGA that is produced by glycolysis from triose phosphate will be unlabelled, whereas half the PGA molecules produced by Rubisco are labelled in the C1 position (Fig. 1b). Thus, the labelling level in PGA is a function of the relative contributions of glycolytic flux and the flux through Rubisco, taking into account the enrichments in the precursors triose phosphate and ribulose-1,5-bisphosphate. The relationship (derived from metabolic and isotopic steady-state equations; see Supplementary Information III) is

$$\text{proportion of PGA from RuBisCO} = \frac{2V_{Rub}}{2V_{Rub} + V_{GAPDH}} = \frac{2F_{PGA(1)}}{F_{CO_2}} \quad (3)$$

where V_{Rub} and V_{GAPDH} are the fluxes through Rubisco and glyceraldehyde 3-phosphate dehydrogenase, respectively; F_{CO_2} and $F_{PGA(1)}$ are the fractional ^{13}C enrichments in CO_2 within the embryos and in the C1 position of PGA, respectively. We determined $F_{PGA(1)}$ from Phe and Tyr carbon position 1 and we estimated F_{CO_2} from label in C1 of valine (Table 2, Fig. 1b). On the basis of the data in Table 2 (using $F_{Phe(1)}$ as well as $F_{Tyr(1)}$) and equation (3) we estimate that the flux through Rubisco is responsible for the production of 37–51% of PGA in the developing embryo. This estimate is a minimum because CO_2 produced by the OPPP is unlabelled, thus rendering the real value for F_{CO_2} smaller than estimated.

We next considered whether any other metabolic routes are possible for the conversion of hexose to fatty acids that could

Table 2 **Refixation of $^{13}CO_2$ by Rubisco in cultured *B. napus* embryos**

Measured metabolite	Corresponding biosynthetic precursor	Proffered labelled precursor		
		$^{13}CO_2$	[1-^{13}C]Ala	[U-$^{13}C_3$]Ala
		Product fractional ^{13}C enrichment		
$F_{Phe(1)}$	$F_{PGA(1)}$	2.5 ± 0.1	1.6 ± 0.1	1.6 ± 0.1
$F_{Tyr(1)}$	$F_{PGA(1)}$	3.0 ± 0.3	2.2 ± 0.3	
$F_{Val(2-5)}$	$F_{PGA(2-3)}$	0.2 ± 0.04	0.08 ± 0.05	
$F_{oleic\ acid(1-18)}$	$F_{PGA(2-3)}$	0.1 ± 0.01	0.1 ± 0.01	
$F_{Val(1)}$	$F_{Pyr(1)}$ (internal CO_2)*	2.6 ± 0.1	8.6 ± 0.1	8.1 ± 0.1

$^{13}CO_2$ was provided as external labelled substrate or was produced inside the developing embryo by metabolism of [1-^{13}C]Ala or [U-$^{13}C_3$]Ala. ^{13}C incorporated into different biosynthetic products from 3-PGA (compare with Fig. 1b) is presented. Fractional ^{13}C enrichment is denoted as $F_{metabolite(carbon\ atoms)}$. Values (means ± s.d., $n = 4$) represent fractional ^{13}C enrichment (above natural ^{13}C abundance) in amino acids and fatty acids as determined by gas chromatography/mass spectrometry. Pyr, plastidic pyruvate. The biosynthetic precursor/product relations are taken from refs 6 and 9.
*For labelling with [1-^{13}C]Ala and [U-$^{13}C_3$]Ala the label in C1 of Val was assumed to represent the ^{13}C enrichment in internal CO_2 (compare with Fig. 1b).

account for our observations. To do this we used elementary flux mode analysis[10,11] applied to the enzymes of glycolysis, the OPPP, the Calvin cycle and fatty-acid synthesis (see Supplementary Information IV). This analysis showed that only the group of elementary flux modes that include the bypass of glycolysis by Rubisco can explain the observed increase in carbon conversion efficiency and labelling results. Three additional sets of flux modes were identified that describe the conventional glycolytic route, the Calvin cycle and the conversion of hexose phosphates to pentose phosphates through the oxidative decarboxylation of hexose with the subsequent formation of PGA through phosphoribulokinase and Rubisco. Linear combinations of the different flux modes showed that increased carbon efficiency is achieved only by increasing flux through Rubisco but comes at the cost of increasing requirement for external (photosynthetic) NADPH. The analysis also shows that with only a small fraction (less than 15%) of the NADPH or ATP required for the Calvin cycle, Rubisco in seeds can carry most of the metabolic flux to oil (see Supplementary Information IV). The flux distributions that are actually available to a developing seed will depend on the amount of light available for generating ATP and NADPH by photosynthetic electron transport. Indeed, as shown in Fig. 2, the ratio of carbon stored in oil to carbon liberated as CO_2 increases linearly with light intensity between 10 and 100 $\mu mol\, m^{-2}\, s^{-1}$.

In addition to demonstrating the operation of the new pathway in *B. napus* and the increased carbon efficiency that it confers, we also assessed the efficiency of carbon metabolism in developing non-green seeds. For two sunflower varieties developing in culture, the oil:CO_2 ratio ranged from 1.2 to 1.6 ($n = 3$ for each variety). This is similar to the ratio expected for the conventional glycolytic pathway to oil (taking into account some CO_2 release from respiration and the OPPP) and is in keeping with our prediction that the increased efficiency conferred by the new pathway requires light and photosystems to provide cofactors.

For green seeds, the presence of glycolysis, the OPPP, Rubisco and photosystems provides alternative metabolic routes that allow adaptations to different environments and thereby maximize the use of both the carbon provided by the mother plant and the light available to the embryo. The survival advantage to plants of the more efficient metabolic flux to carbon storage that we describe might explain why seeds of many species are green and contain substantial Rubisco activity during development despite the absence of sufficient light for the operation of the Calvin cycle. □

Methods

Isotopically labelled substrates

[U-^{14}C]glucose, [U-^{14}C]sucrose, [U-^{14}C]glutamine and [U-^{14}C]alanine were purchased from Amersham Biosciences. $NaH^{14}CO_3$, $NaH^{13}CO_3$, [1-^{13}C]alanine and [U-$^{13}C_3$]alanine were purchased from Sigma-Aldrich.

Embryo culture system

Embryos of *Brassica napus* L (cv. Reston) collected early in the oil accumulation stage were cultured for 3 days in 5 ml liquid medium as described previously[6,9]. Carbon sources were sucrose (80 mM), glucose (40 mM), glutamine (35 mM) and alanine (10 mM) at concentrations mimicking the endosperm liquid in which embryos develop *in planta*.

Measurement of the CO_2 balance for growing embryos

All organic carbon sources were uniformly labelled with ^{14}C by adding [U-^{14}C]sucrose, [U-^{14}C]glucose, [U-^{14}C]glutamine and [U-^{14}C]alanine to the medium, resulting in a specific radioactivity of 1.42 mCi per mol of carbon. Culture flasks were sealed with sleeve stoppers containing two inlets. A 2% $^{14}CO_2$ atmosphere was created inside the flasks by placing a glass vial into the flask containing 18.6 mg $NaH^{14}CO_3$, and injecting HCl directly into the vial to release the $^{14}CO_2$.

Determination of $^{14}CO_2$ efflux

After culture, the flasks were flushed for 2 h with nitrogen at 45 ml min^{-1} with exhaust gas bubbled through a 250-ml wash bottle containing 140 ml of 1 M KOH. The efficiency of the CO_2 trap for $^{14}CO_2$ recovery was on average 99.6% (s.d. = 3.3%). An aliquot (2.5 ml) of the trapping solution was counted by liquid scintillation.

Separation of ^{14}C-labelled compounds

To extract lipids, ^{14}C-labelled embryos were homogenized with a glass microgrinder at 4 °C in 1 ml iso-octane:isopropanol (2:1, v/v). The samples were centrifuged for 5 min at 5,000*g* and the supernatants were pipetted into glass test tubes (lipid fraction). Lipid extraction was repeated three times. To recover proteins, the pellet was extracted twice with 1 ml of 0.01 M sodium phosphate saline buffer (pH 7.4) containing 1 mM EDTA, 10 mM 2-mercaptoethanol, 0.02% sodium azide and 0.0125% (w/v) SDS. After extraction of protein, a fibre/polysaccharide fraction was recovered by hydrolysis of the pellet in 0.5 ml of 67% aqueous sulphuric acid. ^{14}C in each fraction was determined by liquid scintillation counting.

$^{13}CO_2$ labelling

For labelling with stable isotope, embryos were grown for 3 days in a liquid medium as described above in a 2% CO_2 (v/v) atmosphere. CO_2 or alanine were replaced with $^{13}CO_2$, [1-^{13}C]alanine or [U-$^{13}C_3$]alanine, respectively. After growth, lipids and proteins were extracted, and fatty-acid methyl ester and amino acids were obtained as described previously[9]. Amino acids were analysed as *N*,*O*-t-butyldimethylsilyl derivatives and fatty acids as methyl esters by gas chromatograph/mass spectrometer as described earlier[9]. Mass spectra of Phe, Tyr, Val and oleic acid showed significant enrichment of ^{13}C only in the m_1 peaks of each of the fragments observed. The apparent absence of molecules ^{13}C-labelled at multiple positions (m_2, m_3, and so on) allowed the calculation of the fractional ^{13}C enrichments in C1 of Phe, Tyr and Val as follows: $F_{Phe(1)} = m_{1,Phe(1-9)} - m_{1,Phe(2-9)}$; $F_{Tyr(1)} = m_{1,Tyr(1-9)} - m_{1,Tyr(2-9)}$; $F_{Val(1)} = m_{1,Val(1-5)} - m_{1,Val(2-5)}$; $F_{PGA(2-3)} = F_{Val(2-5)} = m_{1,Val(2-5)}$; $F_{PGA(2-5)} = F_{oleic\ acid(1-18)} = m_{1,oleic\ acid(1-18)}$ (fractional enrichment is shown as $F_{metabolite(carbon\ numbers)}$, and mass peak m_X corrected for natural isotope abundance as $m_{X,metabolite(carbon\ numbers)}$). Only in the case of feeding [U-$^{13}C_3$]Ala did the mass spectra of Val and oleic acid reveal molecules to be labelled with ^{13}C at multiple positions (significant abundance of m_2, m_3, and so son). In this case $F_{Val(1)}$ was calculated by subtracting the average ^{13}C enrichment for fragments Val_{1-5} and Val_{2-5} from each other.

Received 13 August; accepted 1 November 2004; doi:10.1038/nature03145.

1. Levin, D. A. The oil content of seeds: An ecological perspective. *Am. Nat.* **108,** 193–206 (1974).
2. Bassham, J. A. *et al.* The path of carbon in photosynthesis. XXI. The cyclic regeneration of carbon dioxide acceptor. *J. Am. Chem. Soc.* **67,** 1760–1770 (1954).
3. Schwender, J., Ohlrogge, J. & Shachar-Hill, Y. Understanding flux in plant metabolic networks. *Curr. Opin. Plant Biol.* **7,** 309–317 (2004).
4. Neuhaus, H. E. & Emes, M. J. Non-photosynthetic metabolism in plastids. *Annu. Rev. Plant Physiol. Plant Mol. Biol.* **51,** 111–140 (2000).
5. King, S. P., Badger, M. R. & Furbank, R. T. CO_2 refixation characteristics of developing canola seeds and silique wall. *Aust. J. Plant Phys.* **25,** 377–386 (1998).
6. Schwender, J., Ohlrogge, J. B. & Shachar-Hill, Y. A flux model of glycolysis and the oxidative pentose phosphate pathway in developing *Brassica napus* embryos. *J. Biol. Chem.* **278,** 29442–29453 (2003).
7. Ruuska, S. A., Schwender, J. & Ohlrogge, J. B. The capacity of green oilseeds to utilize photosynthesis to drive biosynthetic processes. *Plant Physiol.* **136,** 2700–2709 (2004).
8. Goffman, F. D., Ruckle, M., Ohlrogge, J. B. & Shachar-Hill, Y. Carbon dioxide concentrations are very high in developing oil seeds. *Plant Physiol. Biochem.* **42,** 703–708 (2004).
9. Schwender, J. & Ohlrogge, J. Probing *in vivo* metabolism by stable isotope labeling of storage lipids and proteins in developing *Brassica napus* embryos. *Plant Physiol.* **130,** 347–361 (2002).
10. Schuster, S., Fell, D. & Dandekar, T. A general definition of metabolic pathways useful for systematic organization and analysis of complex metabolic networks. *Nature Biotechnol.* **18,** 326–332 (2000).
11. Schuster, S., Dandekar, T. & Fell, D. A. Detection of elementary flux modes in biochemical networks: a promising tool for pathway analysis and metabolic engineering. *Trends Biotechnol.* **17,** 53–60 (1999).

Supplementary Information accompanies the paper on **www.nature.com/nature**.

Acknowledgements This work was supported by grants from the Department of Energy, the National Science Foundation and the USDA. Acknowledgement is also made to the Michigan Agricultural Experiment Station for its support of this research.

Competing interests statement The authors declare that they have no competing financial interests.

Correspondence and requests for materials should be addressed to J.S. (schwend2@msu.edu).